Piezo-optical properties and infrared spectra of Rb_2SO_4 crystals

Vasyl Stadnyk [a], Bohdan Andriyevsky [b*], Ivan Pryshko [a], Leszek Bychto [b], Zenoviy Kohut [c,d], Ulrich Schade [e], Alexander Veber [e], Ljiljana Puskar [e], Ruslan Brezvin[a]

[a] Physics Faculty, Ivan Franko National University of Lviv, Dragomanov str. 19, Lviv 79005, Ukraine
[b] Faculty of Electronics and Computer Sciences, Koszalin University of Technology, Śniadeckich str. 2, PL-75-453, Koszalin, Poland
[c] Lviv Politechnic National University, Lviv 79013, Ukraine
[d] Czestochowa University of Technology, Częstochowa 42-201, Poland
[e] Institute for Electronic Structure Dynamics, Helmholtz-Zentrum Berlin für Materialien und Energie GmbH, Albert-Einstein-Strasse 15, 12489 Berlin, Germany

E-mail addresses:
vasylstadnyk@ukr.net
bohdan.andriyevskyy@tu.koszalin.pl
pryshko_ivan@ukr.net
leszek.bychto@tu.koszalin.pl
zenovij_kohut@ukr.net
ulrich.schade@helmholtz-berlin.de
alexander.veber@helmholtz-berlin.de
ljiljana.puskar@helmholtz-berlin.de
brezvinr@ukr.net

Abstract

The paper deals with the dispersion dependences of birefringence $\Delta n_i(\lambda)$ of the mechanically free and uniaxially clamped Rb_2SO_4 crystal along different crystal-physical axes at room temperature. It was found that the crystal has an insignificant normal dispersion $d(\Delta n_x)/d\lambda\ \chi \leq 0$, and uniaxial compressions σ_m do not change the character, but only the slope of the dependences $\Delta n_i(\lambda)$. Uniaxial loads shift the position of the optical isotropic point both in the short-wavelength (σ_z) and in the long-wavelength part of the spectrum (σ_y). The spectral dependences of the combined piezo-coefficients $\pi^0_{im}(\lambda)$ were calculated and it was found that they have an insignificant dispersion dependence, and the piezo-coefficients π^0_{31} and π^0_{21} are equal to each other in the vicinity of the optical isotropic point at the light wavelength λ = 490 nm. The reflection spectra of Rb_2SO_4 crystals were measured in the infrared range at room temperature using FT-IR spectrometer and synchrotron radiation and the corresponding *ab initio* calculations of the phonon partial density of states and the dielectric function were performed.

Key words: crystal, birefringence, dispersion, uniaxial pressure, piezo-optical coefficients, optical isotropic point, infrared reflection spectra, density functional theory calculations, partial density of states, dielectric function.

Introduction

Today, acousto-optical interactions have a wide practical application. They allow controlling light flows (modulation, changing the frequency or polarization of monochromatic radiation, changing the direction of propagation, etc.), processing information in real time, calculating correlation integrals, and searching for new elements in optoelectronics. These are, first of all, acousto-optical modulators

* corresponding author bohdan.andriyevskyy@tu.koszalin.pl

and deflectors. The latter are used to deploy the light beam along the lines and the platform, similar to the deployment of electrons on the TV screen. To determine the acousto-optical efficiency of a material, it is necessary to determine all components of the tensor of piezo-optical coefficients π_{ik} (POC) (the indices *i* and *k* denote the directions of light polarization and deformation, respectively) is a difficult task [1–8]. For this, interferometric methods are used [9–12], which allow finding all components of the POKC tensor π_{ik}.

In this work, the piezo-optics of rhombic crystals (symmetry class *mmm*) of rubidium sulfate Rb_2SO_4 (RS), which belongs to the crystal group A_2BX_4, was investigated using the interferometric method. Interest in this crystal group is due to the fact that some members of the group have large piezo- and elasto-optical coefficients. For example, the largest POC of the ammonium sulfate crystal [13] are the coefficients π_{11}, π_{12}, and π_{44}, which have values of 11.0, 6.5, and 8.5 Br, respectively (1 Br = 1 Brewster = 10^{-12} m^2/N). For comparison: the largest POC of the model acousto-optical (AO) $LiNbO_3$ crystal have values of π_{13} = 0.78 and π_{44} = 2.25 Br [14], and other representatives of the A_2BX_4 group: ammonium fluoroberylate $(NH_4)_2BeF_4$ [15] and K_2ZnCl_4 have changes in the refractive index n_i, which corresponds to the value of the POC π_{im} ~ 5...7 Br [16].

Crystals of the A_2BX_4 group (A = K, Li, Rb, NH_4, BX_4 = SO_4, BeF_4, $ZnCl_4$) are interesting in that they have an optical isotropic point (OIP), which consists in increasing the symmetry of the optical indicatrix when the spectral range or temperature changes. The transition through OIP is accompanied by a change in the sign of birefringence of the crystal, i.e., its inversion takes place [17-20]. OIP is the result of temperature-spectral deformations of the optical indicatrix of crystals and consists in the fact that for each wavelength only at a certain temperature the transition of the crystal from uniaxial to isotropic or from biaxial to uniaxial state takes place. The presence and temperature dependence of the isotropic state of the crystal is associated with spectral and temperature changes in the refractive indices $n_i(\lambda, T)$ [21-24].

OIP crystals are interesting for the possibility of their use in crystal-optical sensors for measuring temperature and pressure, as well as acousto-optical modulators, especially in the infrared part of the spectrum. For this purpose, we have chosen one of the representatives of this group - the crystal of rubidium sulfate (RS) Rb_2SO_4. Previously, in this crystal at room temperature, it was found that the refractive indices n_z and n_y are close in the visible part of the spectrum, so that at the wavelength λ = 495 nm they intersect at room temperature ($n_z = n_y$ = 1.51705) [25], which indicates the existence OIP along the crystal-physical direction *X*.

The RS crystal is a typical representative of the $ABSO_4$ group, at the temperature of T_c ~ 922 K it undergoes a phase transition (PT) from the pseudohexagonal paraelectric phase *P*-3*m*1 to the orthorhombic ferroelastic phase (space group symmetry D_{2h}^{16} - *Pmcn* [26-28]. Their crystal structure was studied and it was found that the obtained crystals have the *Pnma* symmetry space group with the following refined lattice parameters: *a* = 7.82079(10) Å, *b* = 5.97778(7) Å, and *c* = 10.44040(13) Å. The band energy structure of the crystal is characterized by the band gap of the direct type (E_g = 4.89 eV) and a insignificant dispersion of energy levels. It was found that for the Rb_2SO_4 crystal, as for many other crystals of the A_2BX_4 group, the top of the valence band is formed by the 2*p* states of oxygen atoms, and the bottom of the conduction band is formed by the 4s electrons of rubidium [25].

However, there is no information in the literature about the piezo-optical properties of Rb_2SO_4 crystals and infrared reflection and transmission spectra. Therefore, the purpose of this work is to investigate the piezo-optical coefficients and reflection spectra in the infrared part of the spectrum of crystals, as well as to find out the effect of the cationic substitution $Rb^+ \rightarrow (NH_4)^+ \rightarrow Na^+ \rightarrow K^+$ on the optical-electronic parameters of crystals of the $ABSO_4$ group in order to influence and regulate the spectral and temperature ranges of their existence.

There are few references on the study of infrared spectra of Rb_2SO_4 molecules or molecules in the solid matrices [29, 30]. Three main groups of the absorption maxima in the infrared spectra of Rb_2SO_4 molecules were detected, at about 1100 cm^{-1}, 600 cm^{-1}, and 200 cm^{-1}. [30]. The absorption maxima at 1100 cm^{-1} and 600 cm^{-1} correspond to the stretching and bending vibrations in SO_4^{2-} anions, when the absorption features at about 200 cm^{-1} were assigned to the vibrations in Rb - O bonding. We have not found systematic studies of the infrared absorption and phonon properties of Rb_2SO_4 crystals.

Experimental methods

The investigated crystals were obtained by the method of slow evaporation at room temperature of an aqueous repeatedly recrystallized solution of salts of pure rubidium sulfate Rb_2SO_4. The temperature of the solution was 310 K, which was controlled by a thermostat with an accuracy of 0.5 K. The crystal growth was carried out from a spontaneously formed seed with a pseudo-hexagonal symmetry for 20 days. The obtained crystals were of good optical quality and had the shape of an elongated prism, the size of which was approximately 16 × 11 × 8 mm (Fig. 1).

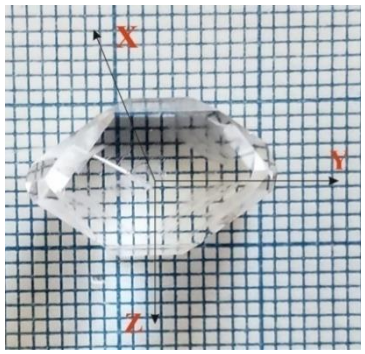

Fig. 1. Habit and setting of the synthesized Rb_2SO_4 crystal

Study of the birefringence Δn of the crystalline sample was carried out by the spectral method, which is based on the analysis of the interference pattern that arises as a result of the decomposition into a spectrum of the white light that has passed through a system of crossed polarizers, between which the sample is placed in a diagonal position and normal to the incident parallel beam of light. The transmission of such a system is described by the relation:

$$I = I_0 \sin^2 \frac{\left(n_i - n_j\right)d}{\lambda} \tag{1}$$

where I_0 and I are the intensities of the input and output beams; λ is wavelength; $(n_i - n_j)$ is the birefringence Δn, d is the thickness of the sample.

The study of birefringence characteristics under action of the uniaxial mechanical pressure was carried out using a special attachment to the cryostat, which makes it possible to compress the crystals using a set of calibrated loads. Then birefringence of the crystal during temperature change or application of uniaxial load is determined as follows:

$$\Delta n(\lambda, T, \sigma) = \frac{k\lambda}{d(T, \sigma)}. \tag{2}$$

In the case of applying a uniaxial stress σ_m, the polarization constants $a_{ij}^{(0)}$ changes by the value Δa_{ij} [12, 22], and then their value will be $a_i = a_{ij}^{(0)} + \pi_{im}\sigma_m$ (π_{im} are absolute piezo-optical coefficients (POC) of the crystal). Since the change in birefringence can be written as, $\delta\Delta n_i = \delta n_j - \delta n_k$, we get the following equation for changing the polarization constants:

$$\Delta a_i = a_i - a_{ij}^{(0)} = \frac{1}{n_i^2} - \frac{1}{n_{0i}^2} = \frac{1}{(n_{0i} + \delta n_i)^2} - \frac{1}{n_{0i}^2} = \frac{n_{0i}^2 - n_{0i}^2 - 2n_{0i}\delta n_i - \delta n_i^2}{n_i^2 n_{0i}^2}. \tag{3}$$

In general, the mechanical stress-induced optical path difference in a crystal is determined by both the induced birefringence $\delta\Delta n_k$ and the induced deformation δd_k of the sample, and it allows one to find the value of the combined POC in the direction of its illumination:

$$\pi_{im}^{*} = 2\frac{\delta(\Delta n_i d_i)}{\sigma_m d_i} - 2\Delta n_i S_{im}. \quad (4)$$

Here S_{im} is the coefficient of elastic compliance, σ_m is the magnitude of the uniaxial mechanical stress, d_i is the thickness of the crystal in the direction of light propagation.

Measurements of the specular reflectance of Rb_2SO_4 single crystal were performed at an incidence angle of 8° using the synchrotron radiation of BESSY II storage ring at the IRIS beamline of HZB (Berlin). The high brilliance of the synchrotron radiation together with a Fourier-transform infrared (FTIR) Bruker Vertex 70/v spectrometer allow for a precise measurement of reflection spectra of the samples by applying a quasi-normal incidence set-up as further described in [31] with a gold film as reference. Measurements were performed using naturally partially polarized IR synchrotron radiation - no additional polarizer was used for the experiment.

The experimental reflection spectra $R(\omega)$ of Rb_2SO_4 crystal were fitted using the Lorentz model of the complex dielectric function $\varepsilon(\omega)$,

$$\varepsilon(\omega) = \varepsilon_\infty + \sum_{j=1}^{N} \frac{\omega_{pj}^2}{\omega_{0j}^2 - \omega^2 - i\gamma_j\omega}, \quad (5)$$

where ε_∞ is the high-frequency dielectric permittivity, ω_p is the plasma frequency, ω_{0j} are the eigen-frequencies of the bonded electrons, γ_j are damping coefficients, and N is the number of oscillators used for fitting [32]. The fitting was performed using the RefFIT software using the model "Reflection and transmission of a multi-layer sample (code -2)" of this package [33].

Theoretical method

The theoretical phonon properties of Rb_2SO_4 crystal were calculated in the framework of the density functional theory using the VASP code [34 – 39] with the projector augmented wave (PAW_PBE) pseudopotentials [40]. The Perdew-Burke-Ernzerhof exchange-and-correlation functional PBE based on the generalized gradient approximation (GGA) [40] has been utilized. The crystal structure of the orthorhombic Rb_2SO_4 (*Pnam*, no. 62) was taken for calculations of the phonon spectra using the density-functional-perturbation theory (DFPT) approach. The electrons $4p^6$ and $5s^1$ for Rb and $3s^2$ and $3p^4$ for S and O were treated as valence ones. The plane wave energy cut-off, 500 eV was used for calculations. The only one *k*-point is chosen in the Monkhorst pack grid 1×1×1 for the Rb_2SO_4 supercell 2×1×2 of the dimensions a = 15.971 Å, b = 10.656 Å, c = 12.203 Å. All the structures were fully relaxed with an energy convergence of 10^{-8} eV. Hellman–Feynman force per atom was minimized to less than 0.005 eV/Å.

Results and discussion

Influence of uniaxial stresses on the birefringent properties of Rb_2SO_4 crystals

The dispersion dependences of the birefringence Δn_i of a mechanically free and uniaxially clamped Rb_2SO_4 crystal along different crystal-physical axes at room temperature are presented in Fig. 2. The following relations between different dispersions of birefringence were found: $d(\Delta n_x)/d\lambda > d(\Delta n_z)/d\lambda > d(\Delta n_y)/d\lambda$. We see that the crystal has a small normal dispersion $\Delta n_i(\lambda)$: $d(\Delta n_x)/d\lambda = -1.2\cdot10^{-6}$ nm^{-1} and $d(\Delta n_z)/d\lambda = -1.6\cdot10^{-6}$ nm^{-1} . In addition, it can be seen that uniaxial compressions σ_m do not change the nature, but only the slope of the curves $\Delta n_i(\lambda)$. So $d(\Delta n_x)/d\lambda \sim -1.1\cdot10^{-6}$ nm^{-1} and $-1.3\cdot10^{-6}$ nm^{-1} for the pressures σ_y and σ_z = 100 bar, respectively; and $d(\Delta n_z)/d\lambda \sim -1.5\cdot10^{-6}$ nm^{-1} and $-1.7\cdot10^{-6}$ nm^{-1} for

pressures σ_y and σ_x = 100 bar, respectively. Uniaxial compressions along the main crystallographic axes change the Δn in absolute value (Fig. 3). Thus, uniaxial compression σ_z leads to a decrease in Δn_x on average $\delta(\Delta n_x) \sim 0.89 \cdot 10^{-4}$, while uniaxial compression σ_y leads to an increase in Δn_x on average $\delta(\Delta n_x) \sim 1.01 \cdot 10^{-4}$. Similar changes were found for Δn_z: load σ_x increases it by $\delta(\Delta i_z) \sim 1.19 \cdot 10^{-4}$, and σ_y decreases it by $\delta(\Delta n_z) \sim 1.34 \cdot 10^{-4}$. This behavior of changes in Δn_y induced by uniaxial compression was confirmed earlier revealed a regularity for crystals of the A_2BX_4 group: uniaxial compressions along mutually perpendicular directions lead to the birefringence changes of different magnitudes and signs.

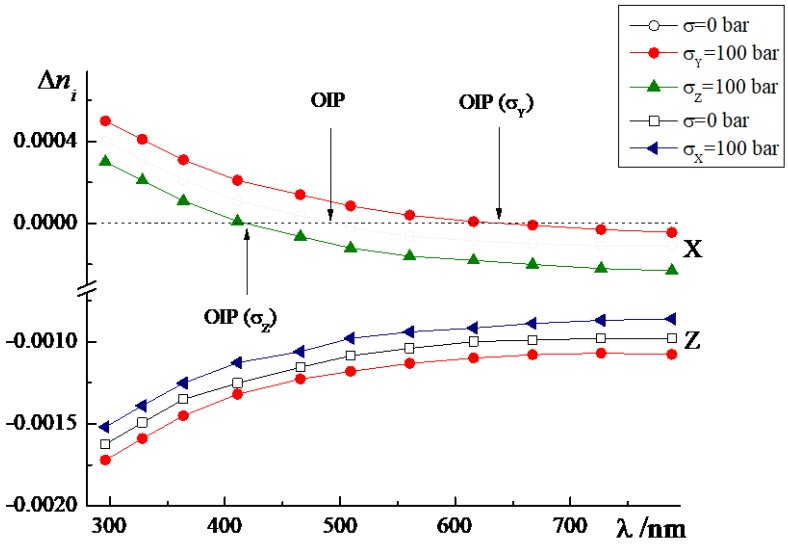

Fig. 2. Dispersion of birefringence of Rb_2SO_4 crystals at room temperature. Light points – mechanically free crystal, colored points – uniaxially loaded along different crystal physical axes. Arrows indicate the position of the optical isotropic point for a mechanically free and uniaxially loaded crystal

We can also see from Fig. 2 the OIP ($\Delta n_x = 0$) at the wavelength λ_0 = 490 nm at room temperature. It was established earlier [41] that in this case, the equality of refractive indices $n_z = n_y = 1.51705$ takes place, which corresponds to OIP. Previously, OIP was found among the group of A_2BX_4 crystals in the isomorphic crystals $(NH_4)_2SO_4$ and $LiNH_4SO_4$ [42, 43]. Since uniaxial loads along the Y and Z axes shift the $\Delta n_x(\lambda)$ curves towards larger and smaller values, the value of the wavelength for which $\Delta n_x = 0$ changes accordingly, which will mean a shift in the position of the IOP along the spectrum. Thus, the OIP will be at the wavelength λ_0 = 420 nm for σ_z = 100 bar and λ_0 = 639 nm for σ_y = 100 bar (Fig. 2). One can estimate the values of spectral-baric shift of the OIP position in RS crystals as a relatively large, $d\lambda_0/d\sigma_z$ = -0.7 nm/bar and $d\lambda_0/d\sigma_y$ = +1.5 nm/bar.

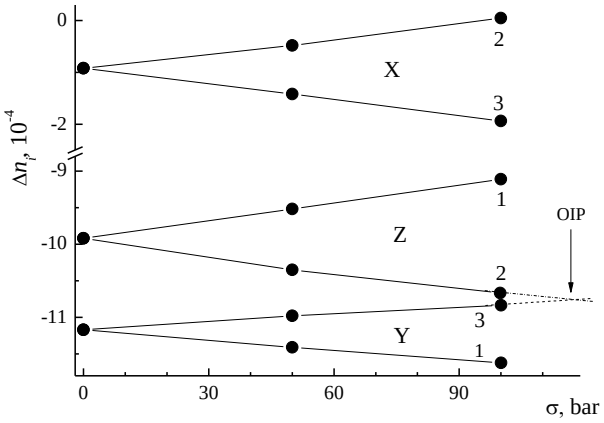

Fig. 3. Baric changes in birefringences Δn_x, Δn_y, and Δn_z of rubidium sulfate crystals obtained at the stresses σ_x (1), σ_y (2), and σ_z (3)

The dependencies $\Delta n_{ij}^{(m)}(\lambda)$ are obtained in a similar way. For this purpose, 45-degree XY-, XZ-, and YZ-cuts of RS crystals were used and subjected to uniaxial compression along the Z-, Y-, and X-directions, respectively. One can see from Fig. 3 that an applying pressure along the Y-axis decreases the value of Δn_z, but an applying pressure along the Z-axis increases the value of Δn_y. By extrapolating the lines $\Delta n_i = f(\sigma_m)$ or solving the equations

$$\Delta n_z\,(\sigma_y = 0) - a\sigma_y = \Delta n_y\,(\sigma_z = 0) + b\sigma_z\,, \qquad (6)$$

where a and b are the coefficients of the baric change of birefringence along the Y- and Z-directions, respectively, it was established that under the simultaneous action of the uniaxial pressures $\sigma_y = \sigma_z = 121$ bar the equality $\Delta n_y = \Delta n_z = -10.77 \cdot 10^{-4}$ will take place, which will correspond to the isotropic state of this crystal.

Since the following relation $\Delta n_y = n_x - n_z$ holds true for the RS crystal, and $\Delta n_z = n_x - n_y$, this will mean that $n_z = n_y$. This corresponds to the emergence of a new "pseudo-isotropic" point. That is, in the case of simultaneous application of a uniaxial load along the crystal physical directions of the Y and Z axes, we can obtain a new OIP at room temperature. Previously, the possibility of induction by simultaneous applying of the uniaxial stress in different crystal-physical directions of new OIPs was discovered in a number of isomorphic crystals of this group, namely K_2SO_4 [44].

According to the definition of piezo coefficients π_{im}, the corresponding baric changes, of the birefringences Δn_k can be written as follows:

$$\delta\Delta n_z^{(y)} \sim (n_y^3\pi_{22} - n_x^3\pi_{12})\sigma_y/2 \quad \text{and} \quad \delta\Delta n_y^{(z)} \sim (n_z^3\pi_{33} - n_x^3\pi_{13})\sigma_z/2\,. \qquad (7)$$

Since in the vicinity of this "pseudoisotropic" point $\sigma_y = \sigma_z$ (Fig. 3) and $n_y = n_z$, we obtain the following combination between absolute piezo-coefficients and refractive indices in the vicinity of the OIR:

$$n_y^3\pi_{22} - n_x^3\pi_{12} \sim n_z^3\pi_{33} - n_x^3\pi_{13}\,. \qquad (8)$$

To further analyze (8), we need to determine the values of the absolute piezo-coefficients π_{im}.

Piezo-optical properties of Rb_2SO_4 crystals

Using formula (4) and the obtained spectral-baric dependences Δn_i for 9 different geometries of the experiment, $\Delta n_x^{(y)}(\lambda)$, $\Delta n_x^{(z)}(\lambda)$, $\Delta n_y^{(x)}(\lambda)$, $\Delta n_y^{(z)}(\lambda)$, $\Delta n_z^{(y)}(\lambda)$, $\Delta n_z^{(x)}(\lambda)$, , as well as, $\Delta n_{xy}^{(z)}(\lambda)$, $\Delta n_{xz}^{(y)}(\lambda)$, $\Delta n_{zy}^{(x)}(\lambda)$ the spectral dependences of the combined piezo-coefficients were calculated (Fig. 4).

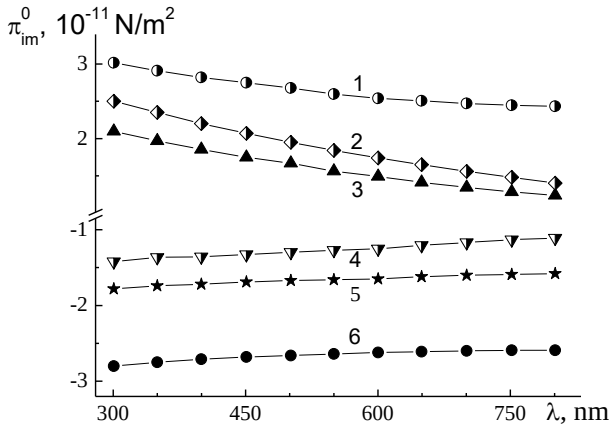

Fig. 4. Dispersion dependences of the combined piezo-optical coefficients $\pi_{im}^{(0)}$ of Rb_2SO_4 crystals at room temperature: 1 – $\pi_{12}^{(0)}$; 2 – $\pi_{23}^{(0)}$; 3 – $\pi_{31}^{(0)}$; 4 – $\pi_{13}^{(0)}$; 5 – $\pi_{21}^{(0)}$; 6 - $\pi_{32}^{(0)}$

A peculiarity of the behavior $\pi_{im}^{(0)}$ of RS crystals is their slight dispersion dependence, while the nature of the dispersion $d\pi_{im}^{(0)}/d\lambda < 0$ corresponds to the dispersion of the refractive indices $dn_i/d\lambda < 0$. The most spectrally dependent is the constant $\pi_{12}^{(0)}$ ($d\pi_{12}^{(0)}/d\lambda = 2.2 \cdot 10^{-2}$ Br/nm), while it changes very little in the spectral range studied ($d\pi_{21}^{(0)}/d\lambda = 0.5 \cdot 10^{-2}$ Br/nm).

Different signs and spectral changes of $\pi_{im}^{(0)}$ indicate that the influence of uniaxial mechanical pressure along the crystal physical axes X, Z, and Y leads to a different nature of changes in the induced birefringence of the RS crystal.

Consider the behavior of the coefficients $\pi_{31}^{(0)}$ and $\pi_{21}^{(0)}$. It can be seen from the graph that for the light wavelength $\lambda = 490$ nm $\pi_{31}^{(0)} \sim |\pi_{21}^{(0)}| \sim 1.67 \cdot 10^{-11}$ N/m^2. That is, not only the symmetry of the optical indicator, but also the symmetry of the tensor of piezo-optical coefficients is increased in the vicinity of the OIP.

The OIP found in Rb_2SO_4 crystal may result from the different pressure and temperature behaviors of the corresponding electron and phonon subsystems. Therefore, a study of the optical properties of the crystal in the infrared range is also of interest.

Infrared reflection spectra of Rb_2SO_4 crystals

It is known that dispersion of the refractive index $n(\lambda)$ of the wide bandgap crystals in the range of optical transparency like RS is determined by the structures of the electron and phonon bands. The structure of phonon bands determines the infrared absorption spectrum of a crystal. That is why the study of phonon properties of RS is necessary for understanding also the piezo-optical properties of the crystal.

The experimental reflection spectra $R(\lambda^{-1})$ (λ^{-1} is wavenumber) of Rb_2SO_4 single crystal are presented in Fig. 5 for two sample's orientations relating the direction of maximum polarization of synchrotron beam. The calculated using RefFIT package the corresponding two components of the real (ε_1) and imaginary (ε_2) parts of dielectric function $\varepsilon(\lambda^{-1})$ ($\varepsilon = \varepsilon_1 + i\varepsilon_2$) are shown in Fig. 6.

The reflectance spectra of Rb_2SO_4 in the frequency range $\lambda^{-1} > 1200$ cm^{-1} indicate no strong vibration resonances (Fig. 5). The maxima of $R(\lambda^{-1})$ and $\varepsilon_2(\lambda^{-1})$ dependences near the wavenumber $\lambda^{-1} = 1150$ cm^{-1} correspond to the stretching vibrations of S – O bonds in SO_4^{2-} anions, when the maximum near the wavenumber $\lambda^{-1} = 610$ cm^{-1} relate to the bending vibrations of S – O bonds in these groups.

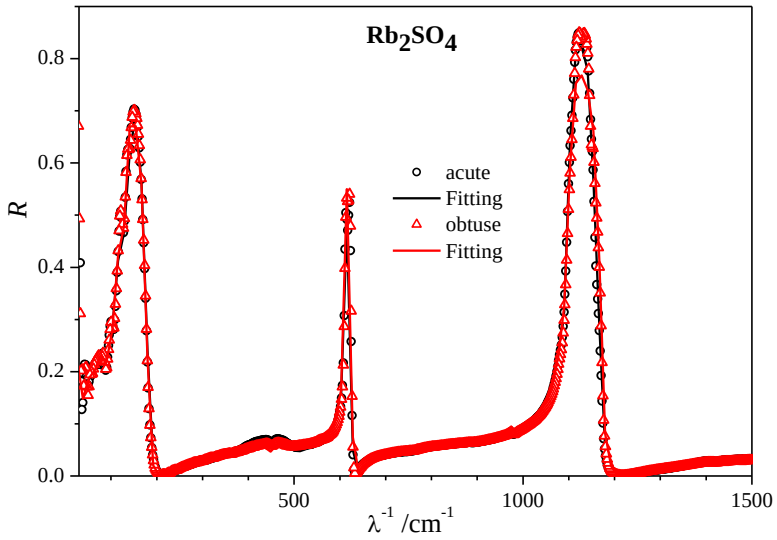

Fig. 5. Reflection spectra $R(\lambda^{-1})$ (λ^{-1} is wavenumber) of Rb_2SO_4 single crystal measured in the infrared range for two orientations of the bisectrix of optical indecatrix (along acute or obtuse bisectrix of optical indicatrix) concerning the direction of the maximum polarization of the synchrotron beam. The fitted reflection spectra $R(\lambda^{-1})$ are indicated by solid lines

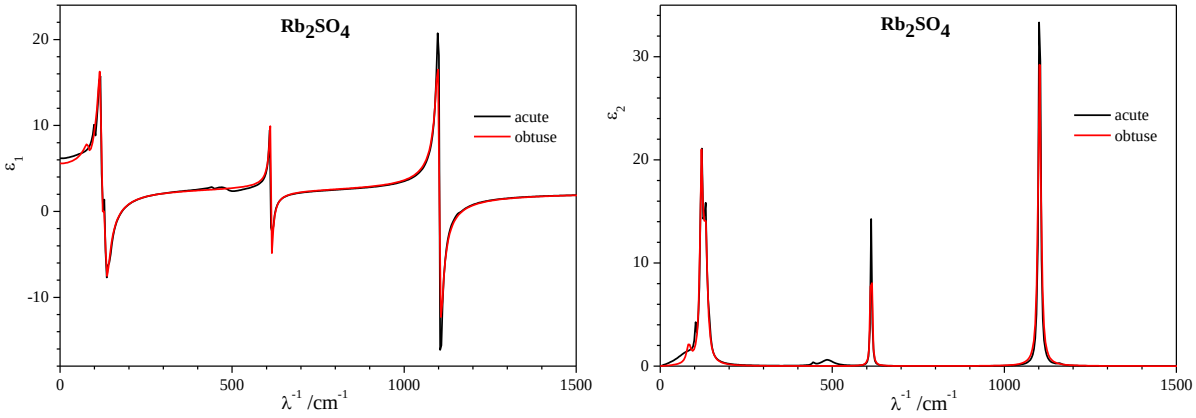

(a) (b)

Fig. 6. Dielectric function $\varepsilon(\lambda^{-1})$ ($\varepsilon = \varepsilon_1 + i\varepsilon_2$,) of Rb_2SO_4, (a) - $\varepsilon_1(\lambda^{-1})$, (b) - $\varepsilon_2(\lambda^{-1})$, in the infrared range fitted using the experimental reflection spectra $R(\lambda^{-1})$ for two orientations of optical indicatrix (along acute or obtuse bisectrix of optical indicatrix) concerning the direction of the maximum polarization of the synchrotron beam

The calculated using VASP package Cartesian components of the imaginary parts of dielectric function of the crystal $\varepsilon_{2x}(\lambda^{-1})$, $\varepsilon_{2y}(\lambda^{-1})$, and $\varepsilon_{2z}(\lambda^{-1})$, are shown in Fig. 7. If to compare the spectral dependences in Fig. 6b and Fig. 7a, a strong similarity in spectral positions of three corresponding groups of maxima of $\varepsilon_{2i}(\lambda^{-1})$ (where the index $i = x, y$, and z correspond to three Cartesian axes) can be observed. This indicates good agreement between the experimental and theoretical *ab initio* results of the positions of maxima of dielectric functions of Rb_2SO_4 single crystal in the spectral range of phonon excitation. Furthermore, the calculated static dielectric permittivities ε_{0i} (Table 1, $i = 1, 2, 3$) are in very good agreement with the experimental real part of the dielectric function ε_1 at the wavenumber $\lambda^{-1} = 0$ (Fig. 6a).

Table 1. The electronic ($\varepsilon_{\infty i}$) and static (ε_{0i}) dielectric permittivities of Rb_2SO_4 crystal calculated using VASP package. The ionic contributions to ε_0, $\varepsilon_0 - \varepsilon_\infty$, are presented in parentheses

ε_∞ (excluding Hartree and local field effects)			ε_0 ($\varepsilon_0 - \varepsilon_\infty$)		
$\varepsilon_{\infty 1}$	$\varepsilon_{\infty 2}$	$\varepsilon_{\infty 3}$	ε_{01}	ε_{02}	ε_{03}
2.3369	2.3214	2.3340	6.1251 (3.7882)	6.3048 (3.9834)	6.6421 (4.3081)

The vibration partial density of states vPDOS of Rb_2SO_4 crystal was calculated using the VASP and Phonopy software and is presented in Fig. 7b. The vPDOS calculated proves that the origin of three infrared absorption bands (Figs. 5, 6b, 7a) is the changes of the dipole moments between different atoms of Rb_2SO_4 induced by the infrared radiation. Really, the infrared absorption takes place in those spectral positions at which the hybridization of vPDOS of different atoms is substantial (Fig. 7b). For this reason, it is remarkable that for the vibration states in Rb_2SO_4, where the hybridization of vPDOS is very small, at the wavenumbers 420 cm^{-1} and 910 cm^{-1} (Fig. 7b), the infrared absorption is absent (Figs. 5, 6b). The latter vibration states may however be active in Raman spectra of the crystal.

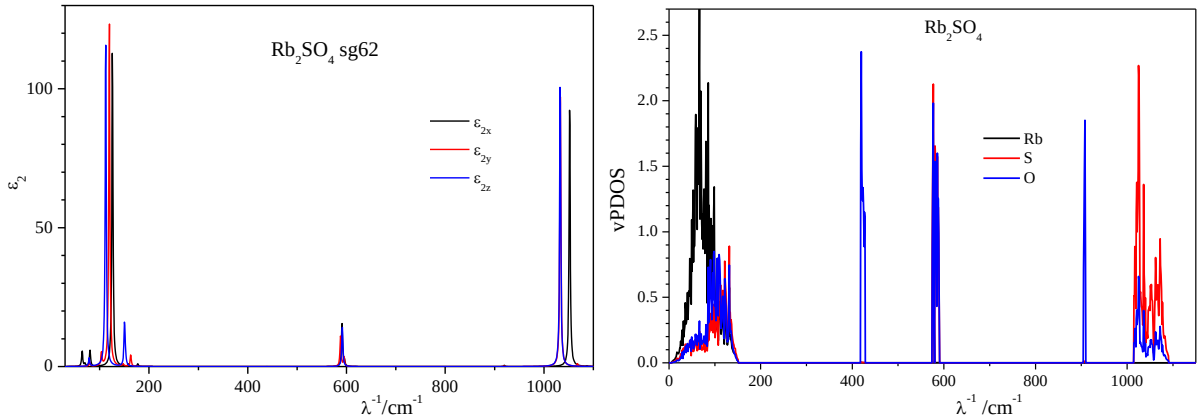

(a) (b)

Fig. 7. (a) Calculated spectra of the imaginary parts of dielectric function $\varepsilon_{2x}(\lambda^{-1})$, $\varepsilon_{2y}(\lambda^{-1})$, and $\varepsilon_{2z}(\lambda^{-1})$, polarized along Cartesian directions *x*, *y*, and *z* of Rb_2SO_4 single crystal at the space group of symmetry no. 62. (b) Calculated vibration partial density of states vPDOS of Rb_2SO_4 single crystal at the space group of symmetry no. 62.

The vPDOS obtained for Rb_2SO_4 single crystal confirm the suggestion derived from the reference studies of the molecular forms of sulfates that the maxima of $R(\lambda^{-1})$ (Fig. 5) and $\varepsilon_2(\lambda^{-1})$ (Fig. 6b) dependences near λ^{-1} = 1150 cm^{-1} correspond to the stretching vibrations of S – O bonds in SO_4^{2-} anions, when the maximum near λ^{-1} = 610 cm^{-1} relate to the bending vibrations of S – O bonds in these groups.

Results obtained for vPDOS indicate that the low-frequency peaks of the reflectance spectrum $R(\lambda^{-1})$ (Fig. 5) and imaginary part of dielectric function $\varepsilon_2(\lambda^{-1})$ (Fig. 6b) at the wavenumber λ^{-1} = 150 cm^{-1} is formed by the vibrations of all atoms, rubidium, sulfur, and oxygen, especially by the vibration of the rubidium cation and sulfate anion due to the ionic bonding Rb^+ - SO_4^{2-}. The more high-frequency peaks of $R(\lambda^{-1})$ and $\varepsilon_2(\lambda^{-1})$ are formed only by the vibrations of sulfur and oxygen atoms. Here, the high-frequency electric field of the infrared radiation does not excite vibrations of the heaviest rubidium atoms.

Conclusions

1. The dispersion dependences of the birefringence $\Delta n_i(\lambda)$ of a mechanically free and uniaxially clamped Rb_2SO_4 crystal along different crystal physical axes at room temperature were investigated in the paper. It was found that the crystal has an insignificant normal dispersion $d(\Delta n_x)/d\lambda \leq 0$, and uniaxial compressions σ_m do not change the character, but only the slope of the curves $\Delta n_i(\lambda)$.

2. It was found that uniaxial stresses shift the position of the optical isotropic point both in the short-wavelength (σ_z) and in the long-wavelength regions of the spectrum (σ_y).

3. The spectral dependences of the combined piezo-coefficients $\pi_{im}^{(0)}(\lambda)$ were calculated and it was found that they have a slight dispersion dependence, while the nature of the dispersion $d\pi_{im}^{(0)}/d\lambda < 0$ corresponds to the dispersion of the refractive indices $dn_i/d\lambda < 0$.

4. It was established that the piezo-coefficients $\pi_{31}^{(0)}$ and $\pi_{21}^{(0)}$ in the vicinity of the optical isotropic point at the wavelength λ = 490 nm are equal to each other, which indicates an increase in the symmetry of the tensor of the piezo-optical coefficients.

5. The precise specular reflection spectra of Rb_2SO_4 crystal were measured in the infrared part of the spectrum 20 - 1500 cm^{-1} at room temperature using FT-IR technique and synchrotron radiation and the complex dielectric function $\varepsilon(\lambda^{-1})$ was obtained.

6. The theoretical DFT-based calculations of Rb_2SO_4 crystal in the energy range of phonon excitations were performed. The calculated positions of maxima of the dielectric function $\varepsilon(\lambda^{-1})$ are found to be in good agreement with the corresponding experimental ones.

7. By comparison of the experimental and theoretical results the origin of the infrared reflection spectral bands was established: the low-frequency band of the reflection spectrum at λ^{-1} = 130 cm^{-1} is formed by the vibrations of rubidium and sulfate ions in Rb – SO_4 ionic bonding, while the reflection maxima at λ^{-1} = 610 cm^{-1} and λ^{-1} = 1100 cm^{-1} are formed by the vibrations of sulfur and oxygen ions in S - O ionic bonding.

Acknowledgement

The study was carried out within the framework of the state budget topic "New broadband materials for detection and control of electromagnetic radiation in dual-purpose devices" (No. 0124U001228). The experimental measurements of infrared spectra of Rb_2SO_4 crystal were performed with infrared synchrotron radiation at the IRIS beamline of the electron storage ring BESSY II at the Helmholtz-Zentrum Berlin für Materialien und Energie. Computer calculations were performed at ICM of Warsaw University, Poland (projects No. g93-1636 and g96-1832) and WCSS of Wrocław University of Technology, Poland (project No. 053).

References

[1] N. Uchida, N. Niizeki, Acoustooptic deflection materials and techniques, *Proc. IEEE* **61** (1973) 1073–1092, https://doi.org/10.1109/PROC.1973.9212

[2] A. Erba, R. Dovesi, Photoelasticity of crystals from theoretical simulations, *Phys. Rev. B* **88** (2013), https://doi.org/10.1103/PhysRevB.88.045121, 045121/1–8

[3] P. P. Natali, L. Montalto, F. Davi, P. Mengucci, A. Ciriaco, N. Paone, D. Rinaldi, Theoretical and experimental evaluation of piezo-optic parameters and photoelastic constant in tetragonal PWO, *Appl. Opt.* **57** (2018) 730–737, https://doi.org/10.1364/AO.57.000730

[4] B. G. Mytsyk, A. S. Andrushchak, D. M. Vynnyk, N. M. Demyanyshyn, Ya P. Kost, A. V. Kityk, Characterization of photoelastic materials by combined Mach-Zehnder and

conoscopic interferometry: application to tetragonal lithium tetraborate crystals, *Opt. Laser. Eng.* **127** (2020), https://doi.org/10.1016/j. optlaseng.2019.105991, 105991/1–8
[5] F. R. Akhmedzhanov, M. I. Elboeva, S. Z. Mirzaev, Exploring of anisotropy of acousto-optic interaction in lead molybdate crystals, *Ultrasonics* **137** (2024), https://doi.org/10.1016/j.ultras.2023.107203, 107203
[6] N. M. Demyanyshyn, B. G. Mytsyk, O. M. Sakharuk, Elasto-optic effect anisotropy in strontium borate crystals, *Appl. Opt.* **53** (2014) 1620–1628, https://doi.org/10.1364/AO.53.001620
[7] N. M. Demyanyshyn, Yu. Suhak, B. G. Mytsyk, O.A. Buryy, Yu. Ya Maksimenko, D. Sugak, H. Fritze, Anisotropy of piezo-optic and elasto-optic effects in langasite family crystals, *Opt. Mater.* **119** (2021), https://doi.org/10.1016/j. optmat.2021.111284, 111284/1–7
[8] R. W. Dixon, M. G. Cohen, A new technique for measuring magnitudes of photoelastic tensors and its application to lithium niobite, *Appl. Phys. Lett.* **8** (1966) 205–207, https://doi.org/10.1063/1.1754556
[9] R. W. Dixon, Photoelastic properties of selected materials and their relevance for applications to acoustic light modulators and scanners, *J. Appl. Phys.* **38** (1967) 5149–5153, https://doi.org/10.1063/1.1709293
[10] D. A. Pinnow, Guidelines for the selection of acoustooptic materials, *IEEE J. Quant. Electron.* **QE6** (1970) 223–238, https://doi.org/10.1109/JQE.1970.1076441
[11] G. A. Coquin, D. A. Pinnow, A. W. Warner, Physical properties of lead molybdate relevant to acousto-optic device applications, *J. Appl. Phys.* **42** (1971) 2162–2168, https://doi.org/10.1063/1.1660520
[12] T. S. Narasimhamurty, Photoelastic and Electro-Optic Properties of Crystals, Springer, 1981, https://doi.org/10.1007/978-1-4757-0025-1. [16] L. Bergmann, Der Ultraschall und seine Anwendung in Wissenschaft und Technik, Zürich, 1954
[13] B. Mytsyk, V. Stadnyk., N. Demyanyshyn, Ya. Kost, P. Shchepanskyi, Photoelasticity of ammonium sulfate crystals, *Opt. Mater.* **88** (2019) 723–728, https://doi.org/10.1016/j.optmat.2018.12.005
[14] T. Azuhata, M. Takesada, T. Yagi, A. Shikanai, S. F. Chichibu, K. Torii, A. Nakamura, T. Sota, G. Cantwell, D. B. Eason, C. W. Litton, Brillouin scattering study of ZnO, *J. Appl. Phys.* **94** (2003) 968–972, https://doi.org/10.1063/ 1.1586466
[15] B. Mytsyk, V. Stadnyk, N. Demyanyshyn, P. Shchepanskyi, Ya. Kost. *Opt. Mater.* **148** (2024) 114880. https://doi.org/10.1016/j.optmat.2024.114880
[16] V. Yo Stadnyk, M. O. Romanyuk, B. V. Andriyevsky, Z. O. Kogut, Baric changes in refractive indices of K_2ZnCl_4 crystals, *Opt. Spectrosc.* **108** (2010) 753–760, https:// doi.org/10.1134/S0030400X10050139
[17] M. A. Hobben. *Acta Cryst*. **A24** (1968). https://doi.org/10.1107/S0567739468001440
[18] C. Schwartz, D. S. Chemla, B. Ayrault, R. C Smith. *Opt. Commun.* **5** (1975), https://doi.org/10.1016/0030-4018(72)90089-2
[19] G. C. Bhar. *J. Phys. D.: Appl. Phys*. **13** (1980), https://doi.org/10.1088/0022-3727/13/3/018
[20] S.C. Abrahams, J. L. Bernstein. *J. Chem. Phys*. **52** (1970), https://doi.org/10.1063/1.1672831
[21] S.C. Abrahams, J. L. Bernstein. *J. Chem. Phys.* **59** (1973), https://doi.org/10.1063/1.1680242
[22] O. S. Kushnir, P. A. Shchepanskyi, V. Yo. Stadnyk, A. O. Fedorchuk. *Opt. Mater.* **95 (**2019) 109221. https://doi.org/10.1016/j.optmat.2019.109221
[23] V. Yo. Stadnyk, R. S. Brezvin, M. Ya. Rudysh, P. A. Shchepanskyi. *Opt. Spectrosc.* **117** (2014). https://doi.org/10.1134/S0030400X14110216
[24] V. Yo. Stadnyk, M. O. Romanyuk, R. S. Brezvin. *Ferroelectrics* **192** (1997). https://doi.org/10.1080/00150199708216190

[25] M. Ya Rudysh, I. A. Pryshko, P. A. Shchepanskyi, V. Yo Stadnyk, R. S. Brezvin, Z. O. Kogut. *Optik* **269** (2022) 169875. https://doi.org/10.1016/j.ijleo.2022.169875
[26] P. E. Tomaszewski. *Phase Transit.* **38** (1992). https://doi.org/10.1080/01411599208222899.
[27] O. Muller, R. Roy. *The Major ternary structural families*, Springer-Verlag, Berlin; Heidelberg; (1974). https://doi.org/10.1180/minmag.1975.040.310.16
[28] L. Vinchel, G. Vinchel. *Optical properties of synthetic minerals*. Mir, Moscow (1967)
[29] H. Takahashi, S. Meshitsuka, K. Higasi, Infrared spectra and lattice vibrations of alkali and alkaline-earth metal sulfates, *Spectrochim. Acta A: Molec. Spectrosc.* **31** (1975) 1617 – 1622
[30] A. A. Belyaeva, M. I. Dvorkin, L. D. Shcherba, Vibrational spectra and structure of the molecules of alkali metal sulfates isolated in inert gas matrices, *Zhurnal Strukturnoi Khimii* **21** (1980) No. 6 50-59
[31] U. Schade, M. Ortolani, J. Lee, THz experiments with coherent synchrotron radiation from BESSY II, *Synchrotron Radiat. News* **20** (2007) 17-24. https://doi.org/10.1080/08940880701631351
[32] P. Y. Yu, M. Cardona, *Fundamentals of Semiconductors*, Springer Heidelberg Dordrecht London New York, 2010.
[33] B. Kuzmenko, Kramers-Kronig constrained variational analysis of optical data, *Rev. Sci. Instrum.* **76** (2005) 083108
[34] G. Kresse, J. Hafner, Ab initio molecular dynamics for liquid metals, *Phys. Rev. B* **47**(1993) 558-561. https://doi.org/10.1103/PhysRevB.47.558
[35] G. Kresse, J. Hafner, Ab initio molecular-dynamics simulation of the liquid-metal-amorphous-semiconductor transition in germanium, *Phys. Rev. B* **49** (1994) 14251-14269. https://doi.org/10.1103/PhysRevB.49.14251
[36] G. Kresse, J. Furthmüller, Efficiency of ab-initio total energy calculations for metals and semiconductors using a plane-wave basis set, *Comput. Mater. Sci.* **6** (1996) 15-50. https://doi.org/10.1016/0927-0256(96)00008-0
[37] G. Kresse, J. Furthmüller, Efficient iterative schemes for ab initio total-energy calculations using a plane-wave basis set, *Phys. Rev. B* **54** (1996) 11169-11186. https://doi.org/10.1103/PhysRevB.54.11169
[38] P. E. Blöchl, Projector augmented-wave method, *Phys. Rev. B* **50** (1994) 17953-17979. 10.1103/physrevb.50.17953
[39] G. Kresse, D. Joubert, From ultrasoft pseudopotentials to the projector augmented-wave method, *Phys. Rev. B* **59** (1999) 1758-1775. https://doi.org/10.1103/PhysRevB.59.1758
[40] J. P. Perdew, A. Ruzsinszky, G. I. Csonka, O. A. Vydrov, G. E. Scuseria, L. A. Constantin, X. Zhou, K. Burke, Restoring the density-gradient expansion for exchange in solids and surfaces, *Phys. Rev. Lett.* **100** (2008) 136406. https://doi.org/10.1103/PhysRevLett.100.136406
[41] V. M. Gaba, *Acta Phys. Pol. A* **117** (2010) 129-132. https://doi.org/10.12693/APhysPolA.117.129
[42] B. Andriyevsky, W. Ciepluch-Trojanek, V. Stadnyk, M. Tuzyak, M. Romanyuk, V. Kurlyak. *J. Phys. Chem. Solids* **68** (2007). https://doi.org/10.1016/j.jpcs.2007.05.017
[43] V. Yo. Stadnyk, V. M. Gaba, B. V. Andrievskii, Z. O. Kogut, *Physics of the Solid State* **53** (2011) doi 10.1134/s106378341101029x
[44] B. G. Mytsyk, Ya. P. Kost', N. M. Demyanyshyn, V. M. Gaba, O. M. Sakharuk, Study of piezo-optic effect of calcium tungstate crystals by the conoscopic method. *Opt. Mater.* **39** (2015) 69-73. https://doi.org/10.1016/j.optmat.2014.10.066